Advances in Organic All-Optical Photorefractive Materials

*Yingliang Liu, Haiyan Pei, Li Zhang, Jun Shi, Shaokui Cao**

Summary: Organic all-optical photorefractive (PR) materials will soon become an interesting topic owing to the convenient signal-writing without the application of external electrical field and poling, even without any photosensitizer. In this paper, organic all-optical PR materials synthesized in our laboratory have been systematically summarized including organic monolithic PR molecular glasses with a linear or hyperbranched chemical structure such as organic carbazole/triphenylamine-based amorphous compounds, and PR polymers with a non-conjugated main chain (NCMC) such as polymethacrylates, polyphosphazenes and polynorbornenes. Much progress has been made not only in the synthesis strategy of organic all-optical materials but also in understanding the primary mechanism of all-optical PR effect in organic materials. It is believed that the outcoming of organic all-optical PR materials will broaden the application fields of organic PR materials.

Keywords: all-optical; monolithic molecular glass; photorefractive; postfunctionalization

Organic photorefractive (PR) materials which combine the photoconductivity and the optical nonlinearity (NLO) have been widely studied on account of the easily tunable performance of organic materials, the easy fabrication of PR devices, the low cost and their potential applications in holographic data storage, image processing, non-destructive testing, photoswitching, real-time display, etc.[1] Much progress has been made in material synthesis, device fabrication and physical mechanism about organic PR materials, which have been able to be applied to such as rewritable three-dimensional data storage,[2] updatable three-dimensional display[3] and bistable device.[4] Generally, the PR effect is based on a combination of photoconducting and electro-optic properties and can lead to high refractive index variation under illumination. The response wavelenght ranges from the visible region to the near-infrared reagion, including the organism-transparent wavelenghts near 800 nm and the telecommunication wavelengths of 850 nm, 1310 nm, 1550 nm. According to the PR mechnism, the refractive index change might come from charge seperation,[5] photochemical reaction,[6] phase change and even mobility of ionic liquids inside the materials.[7] Organic PR materials based on charge seperation possesses the following processes: (1) the charge carriers are generated in the high-intensity regions of interference pattern with two laser beams intersecting inside the PR materials, (2) one type of carrier is transported from the high-intensity region to the low-intensity and trapped, (3) the trapped charge carriers create an alternating internal space-charge field, namely internally built-up electric field, (4) the space-charge field induces a refractive index grating via the electro-optic effect because the PR materials are electro-optic. As a result, the initial light distribution is optically encrypted in the form of a refractive-index pattern inside the PR material. Compared to inorganic PR materials, organic PR materials have unique characteristics of an orientational contribu-

School of Materials Science and Engineering, Zhengzhou University, Zhengzhou 450052, P. R. China
Fax: +86-371-6776-3561;
E-mail: caoshaokui@zzu.edu.cn

tion to the refractive-index modulation, which affords a larger refractive-index change. This orientational enhancement effect is derived from the orientation of organic PR chromophore at room/operating temperature under the total influence of internal and external electric field. Consequently, the PR chromophore will have a spatially modulated orientation in magnitude and in direction. This PR chromophore is usually designed as aromatic π-electron systems unsymmetrically end-capped with electron donating and accepting groups to impart the directional bias according to the regulation of second-order NLO chromophores suggested by Ouda and Chemla.[5] Therefore, the dipole moment of the PR chromophore plays an important role in the PR effect of organic PR materials although the hyperpolarizability and the polarizability anisotropy of PR chromophores also need to be taken into account, especially in the orientational enhancement effect.

As one of second-order NLO materials, it is neccessory for organic PR chromophore not to have a center of symmetry. Simutanueously, the non-centrosymmetric PR chromophore must be arranged inside the PR materials in such a manner that the bulk material also does not have an effective center of symmetry in order to exhibit the bulk photorefractivity. Therefore, poling and an external electric field are usually necessary to obtain an excellent photorefractive performance from PR bulk materials. Besides, except for organic PR chromophores, other components including photoconductors, photosensitizers and even plastisizers, which perform different functionality in the PR bulk materials, are also needed in common occasion. Interestingly, some of organic multifunctional PR materials including polymeric PR materials and monolithic molecular glasses that we have prepared in our lab can show a good PR performance without poling and application of an external electric field, even without any photosensitizer and plasticizer, which are defined as all-optical PR materials. Out of question, all-optical PR materials will broaden the application fields of organic PR materials. At the same time, many new problems are encountered including all-optical PR chromophore design and novel physical theory about all-optical PR effect. This paper will mainly summarize our work about organic all-optical photorefractive materials including monolithic PR molecular glasses and polymer PR materials, although the photorefractive performance under external electric field is mentioned.

Monolithic PR Molecular Glasses

According to the basic design rule, a PR chromophore generally has an aromatic π-electron system asymmetrically end-capped with electron donating and accepting groups as shown in Scheme 1, together with the absence of a molecular center of symmetry. In our work, carbazole or triphenylamine is introduced as a donor into the PR chromophore, while nitro, cyano or ester groups connected with aromatic rings in some occasion act as an acceptor. Usually, this kind of push-pull molecular structure including a donor and an acceptor has a permanent dipole moment, which may induce the molecular aggregation although they have an intrinsical electro-optic response under external electric fields. In other words, these molecules are commonly crystalline compounds. This will cause the existence of many crystalline microparticles in existence inside the PR devices which is the main

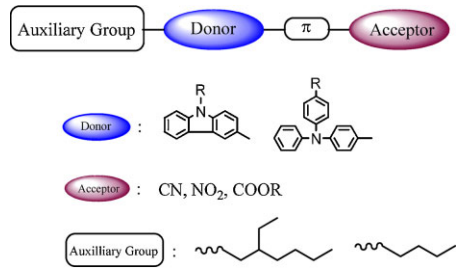

Scheme 1.
Basic molecular design for a PR chromophore.

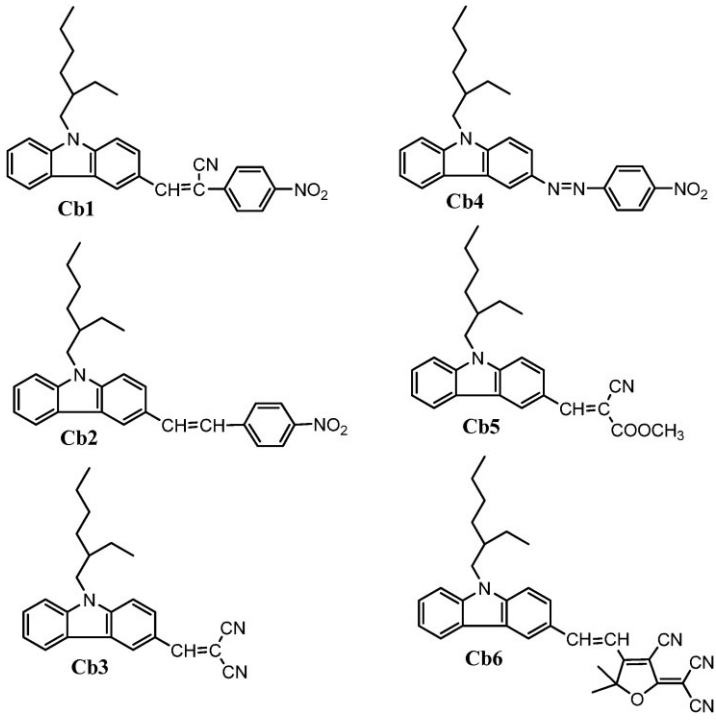

Scheme 2.
Monolithic molecular glasses with carbazole as a donor.

reason for light-scattering. It is also the main issue which induces the long response time of organic PR devices compared to organic monolithic molecular glasses, since the dissociation and reorientation of the PR molecules in the aggregation state is difficult. Therefore, an auxiliary group is often introduced into the PR chromophore in order to block the molecular aggregation and to make the PR molecules transparent affording the transparent ability and to give the appropriate response time for the PR films, together with regulating the glass transition temperature (T_g) of the amorphous compounds.

The monolithic molecular glasses with carbazole as a donor used in this study are shown in Scheme 2.[8] In this series of monolithic molecular glasses, a melting endotherm together with the recrystallization exotherm are observed for compounds **Cb1** and **Cb6** with the plane chemical structure of the electron-donating carbazole and the strong electron-accepting ability in the acceptor part. The other PR compounds do not have any recrystallization exotherms besides the introduction of 2-ethylhexanyl group with a branched chemical structure. As shown in Table 1, their T_g values measured by DSC change from $-2\,^{\circ}C$ to $69\,^{\circ}C$ indicating the ability to form a glassy state. Due to the introduction

Table 1.
Thermal and optical properties of carbazole-based monolithic molecular glasses.[a]

Sample	λ_{max}/nm	T_g/°C	M_p/°C	T_{rec}/°C	Γ_{633}/cm^{-1}
Cb1	410	23	151	51.9	266
Cb2	409	2	141	/	10
Cb3	406	−2	81	/	8
Cb4	437	−2	79	/	8
Cb5	396	0	77	/	11
Cb6	500	69	182	130	/

[a]The Γ_{633} is the coupling gain measured by TBC from the doped PR films with a photosensitizer of 1% or 2% TNF except for **Cb1** without any photosensitizer. λ_{max} is the absorption maximum wavelength; T_g is the glass transition temperature; M_p is the melting point; T_{rec} is the recrystallization temperature.

of different acceptors, the absorption maxima measured by UV-vis spectroscopy vary from 396 nm to 500 nm because of the internal charge transfer between the electron-donating carbazole nucleus and the electron-accepting methine or azo groups. Compound **Cb6** has the highest λ_{max} derived from the strong electron-withdrawing ability of the tricyanofuran group. Such dipolar features will afford a near-infrared photorefractive response, which will be investigated in our future work.

The PR performance was characterized at room temperature by two-beam coupling (TBC) and four-wave-mixing (FWM) experiments with 633 nm laser as a light source using the experimental setup shown in Figure 1. Compound **Cb1** exhibits the best PR performance due to the highest coupling gain of 266 cm^{-1} at electric field of 42 V/μm without any photosensitizer. In this case, the FWM efficiency was 5% at electric field of 27 V/μm. It was assumed that this excellent photorefractive performance comes from the low T_g value and the good asymmetrical chemical structure through the lateral introduction of a cyano group in the double bond (C=C). The coupling gains of other compounds are only around 10 cm^{-1} even with the addition of 1% or 2% TNF as a photosensitizer.

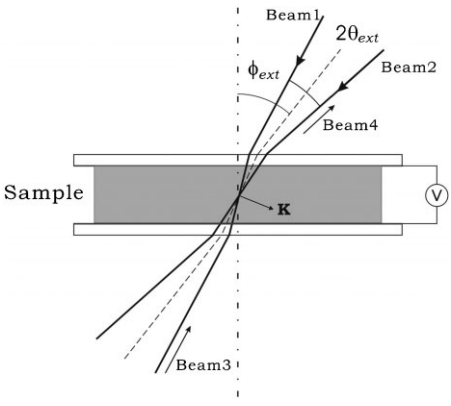

Figure 1.

Experimental setup for TBC and FWM. Only beam 1 and beam 2 are present in TBC experiment, which are *p*-polarized laser beams. Beam 3 is the *s*-polarized probe beam and beam 4 is the diffractive beam. $\phi_{ext} = 35^{o}$ is the tilted angle of the symmetric axis of the two incident beams with respect to the sample normal, and $2\theta_{ext} = 20^{\circ}$ is the external interbeam angle. K is the grating wave vector. V is an applied external electric field.

The monolithic molecular glasses with triphenylamine as a donor are shown in Scheme 3.[9] Notably, this series of compounds **TPA1**-**TPA5** has no melting endotherm and recrystallization exotherm except that compound **TPA6** has a melting endotherm at 197 °C and a recrystallization exotherm at 143 °C as shown in the DSC curve in Figure 2, although there is no branched aliphatic chain to be introduced as an auxiliary group instead of the linear aliphatic chain, *n*-butyl group. This indicates that the triphenylamine-based PR compounds can form a more stable glassy state than the carbazole-based PR compounds owing to the nonplanar three-dimensional chemical structure of triphenylamine. As shown in Table 2, the T_g values of this series of monolithic molecular glasses measured by DSC vary from −14 °C to 77 °C. The absorption maxima measured by UV-vis spectroscopy are also red-shifted from 425 nm to higher than 500 nm. Interestingly, TBC results suggested that the undoped PR film of compound **TPA1** has a coupling gain of 52 cm^{-1} at zero electric field without any photosensitizer and poling although the coupling gain is increased to 165 cm^{-1} with applying external electric field of 40 V/μm. The TBC signal from the undoped PR film of compound **TPA1** is illustrated in Figure 3. This phenomenon is defined as an all-photorefractive effect. In addition, compound **TPA2** shows the same phenomenon as compound **TPA1** in despite of the low coupling gain of 18 cm^{-1} at zero electric field. This all-optical PR effect will simplify the writing process of digital or image information into the PR devices to a great extent. At least, an external electric field will not be needed although the PR devices show a better PR performance under its existence. At the same time, conductive ITO-glasses, which are needed for applying an external electric field on the PR devices, are abandoned. Without question, this

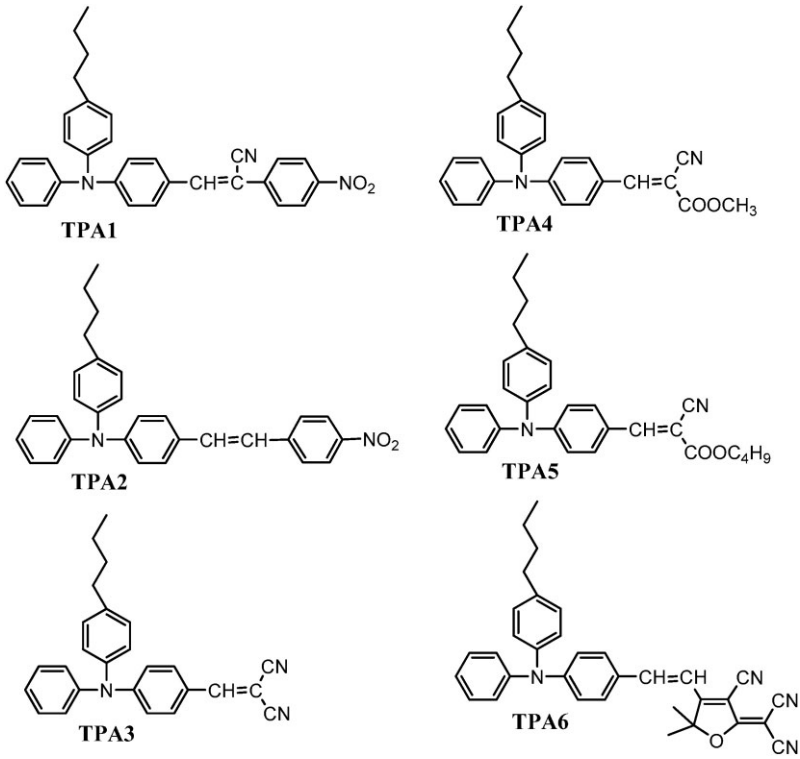

Scheme 3.
Monolithic molecular glasses with triphenylamine as a donor.

reading-in simplification of digital or image information will broaden the application fields and lower the fabrication cost of PR devices. Compounds **TPA3**, **TPA4**, **TPA5** and **TPA6** have no all-optical photorefractive effect while compounds **TPA3** and **TPA4** have a coupling gain of $60\,cm^{-1}$ at $20\,V/\mu m$ and $35\,cm^{-1}$ at $30\,V/\mu m$, respectively. Similar to compound **Cb6** in the carbazole-based monolithic molecular glasses, compound **TPA6** possibly shows a near-infrared photorefractive response, which will also be a part of our future work.

Hyperstructured monolithic molecular glasses with cyclotriphosphazene as the

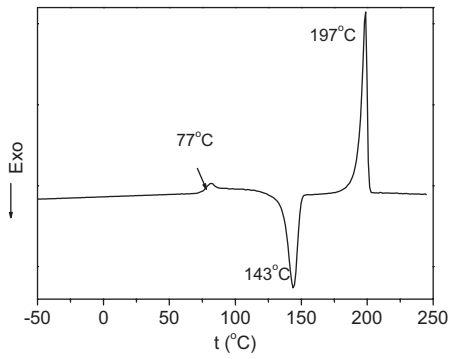

Figure 2.
DSC curve of monolithic molecular glass TPA6.

Table 2.
Relative data to triphenylamine-based monolithic molecular glasses.

Sample	λ_{max}/nm	T_g/°C	Γ_{633}/cm^{-1} (V/μm)
TPA1	452	20	52 (0), 165 (40) [a]
TPA2	432	5	18 (0) [a]
TPA3	436	13	60 (20) [b]
TPA4	425	−2	35 (30) [b]
TPA5	425	−14	/
TPA6	>500	77	/

Note: λ_{max} is the absorption maximum wavelength; T_g is the glass transition temperature; Γ_{633} is the coupling gain from TBC.[a]the data obtained from nondoped PR films without any photosensitizer;[b]the data obtained from doped PR films with a photosensitizer of 0.5% TNF.

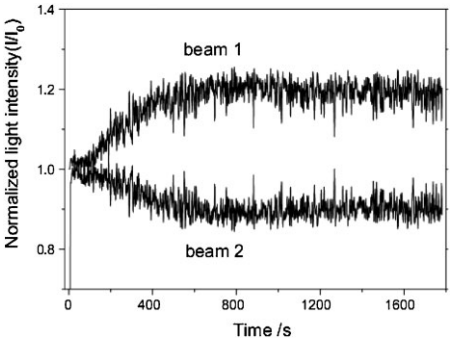

Figure 3.
TBC signal from nondoped PR film of **TPA1** at zero electric field without any photosensitizer and poling.

molecular core were also prepared as shown in Scheme 4.[10] Six carbazole groups are firstly grafted onto the cyclotriphosphazene core as charge-transport agents via nucleophilic substitution affording a hyperbranched structure of compound **CTP0** through a complete substitution of the chlorine atoms in hexachlorocyclotriphosphazene by *N*-hydroxyethylcarbazole. In contrast to linear compounds, such as the carbazole/triphenylamine-based monolithic molecular glasses, the hyperbranched molecular structure provides many terminal carbazole groups for further functionalization. Various electron-withdrawing groups can be incorporated into the hyperbranched molecules by extension of conjugated structure of carbazole to get molecular EO nonlinearity. Herein, two hyperbranched compounds **CTP1** and **CTP2** were respectively synthesized through functionalization of one carbazole group and two carbazole groups in the

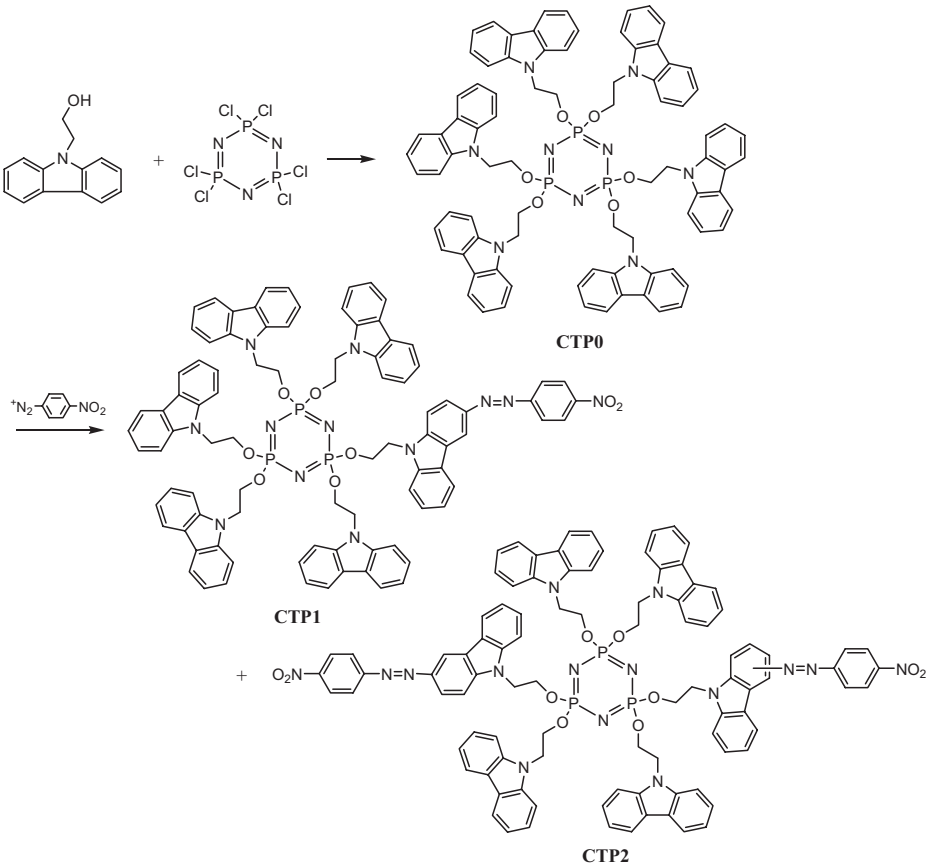

Scheme 4.
Hyperstructured monolithic molecular glasses with cyclotriphosphazene as a molecular core.

Table 3.
Relative data to hyperbranched monolithic molecular glasses.

Sample	λ_{max}/ nm	T_g^1 (°C)	T_g^2 (°C)	Γ_{633}/cm^{-1} (V/μm)[a]
CTP0	345	57	/	/
CTP1	430	82	31	102 (0)
CTP2	430	90	40	214 (0)

Note: T_g^1 is the glass transition temperature of the molecules; T_g^1 is the glass transition temperature of the molecular composites; λ_{max} is the absorption maximum wavelength; Γ_{633} is the coupling gain from TBC.[a]the data obtained from the PR films with 30% *N*-ethylcarbazole and without any photosensitizer and poling.

hyperbranched compound **CTP0**. The absorption maxima of compounds **CTP1** and **CTP2** are red-shifted to 430 nm from 345 nm of compound **CTP0** as shown in Table 3. The introduction of a flexible spacer between the molecular core and carbazole group alleviates the steric hindrance and lowers the T_g value. Because of the introduction of only two methylene units, compounds **CTP0**, **CTP1** and **CTP2** have a relative high T_g, which is 57 °C, 82 °C and 90 °C, respectively. However, the DSC measurement indicated that these three compounds stayed in amorphous state.[10]

In order to achieve a lower T_g near room temperature, 30 wt% of *N*-ethyl-carbazole (ECZ) was added as a plasticizer. The T_g values of the resultant molecular composites were decreased to 31 °C for composite **CTP1** and 40 °C for composite **CTP2**. These two composite samples were kept unpoled and directly used for PR measurements. The TBC measurement suggested that the coupling gains of composite **CTP1** and composite **CTP2** at zero electric field without any photosensitizer are 102 cm^{-1} and 214 cm^{-1}, respectively. The diffraction efficiencies measured by FWM are 24% and 31%, respectively. The composite **CTP2** possessed the best all-optical PR performance in all PR devices which we fabricated. It was assumed that the synergism of the photoassisted poling of the azo dye and the longitudinal space charge field may be responsible for the all-optical TBC effect in composite **CTP2**. The repeated *trans-cis-trans* photoisomerization induced by a polarized light allows the PR chromophore to rotate more easily and to orientate at the polarized dimension. Consequently, when the sample was illuminated by the interference pattern, a periodic space charge field can still arise at a zero electric field although no prepoling was carried out.

Polymer PR Materials

PR polymers are another interesting subject because the diverseness of polymer chemistry allows us to design a variety of polymer systems and to optimize their comprehensive properties for practical applications. However, the direct polymerization from a functionalized monomer normally gives a polymer with low molecular weight owing to both the bulkiness of the monomer and the side effect of the functional group,[11,12] which is not beneficial to the film-forming property. Therefore, postfunctionalization strategy becomes a facile approach to synthesize PR polymers with a high molecular weight. The PR chromophore could then be introduced into a reactive precursor polymer without exposing the chromophore to aggressive polymerization condition.[13,14] Additionally, fully/multi-functionalized PR polymers have attracted much attention in recent years in order to avoid low stability due to phase separation, diffusion and volatilization of PR polymeric composites.[1] All the functional entities for PR effect are covalently bound to the polymers, affording good morphological stability and PR properties. While, fully/multi-functionalized PR polymers almost consist a conjugated main chain, which is prepared by complicated synthetic processes. For practical application, fully/multi-functionalized polymers with a non-conjugated main chain (NCMC) structure become a present challenge. Recent progress in organic monolithic PR molecular glasses, which are generally prepared by a simple synthetic route, provides a significant probability for the molecular design of fully/

multi-functionalized NCMC polymers. The excellent PR performance and the synthetic ease of organic monolithic PR molecular glasses make fully/multi-functionalized NCMC polymers to become promising PR materials, especially for all-optical PR NCMC polymers.

Three series of PR NCMC polymers including polymethacrylates, polyphosphazenes and polynorbornenes were synthesized due to the optical transparency of their backbone and the ease of synthesis. Polymethacrylates and polyphosphazenes with PR chromophore were prepared by postfunctionalization approach. Polynorbornenes were presented by the direct polymerization of PR monomers with a polymerizable norbarnene via ring-opening metathesis polymerization (ROMP) under Grubbs I catalyst.

Precursor polymethacrylates **P0** with different alkylene chain length between the main chain and carbazole moiety were synthesized as photoconductive polymers by conventional radical polymerization of methacrylate monomer bearing a carbazole group.[15–17] Then, PR polymethacrylates **P1**–**P6** bearing azo group were prepared through post-azo-coupling reaction of precursor polymers **P0** and corresponding diazonium salt according to the synthetic route **A** in Scheme 5. PR polymethacrylates **P7**-**P9** were synthesized in turn by Vilsmeier reaction and Knovenagel reaction to introduce the methine PR chromophore according to the synthetic route **B** in Scheme 5. The results in Table 4 indicate that the content of NLO chromophore ranges from 25% to 102% with different reaction conditions. DSC results showed that polymers **P1**–**P4** have a higher T_g value from 124 °C-160 °C resulting from the short aliphatic chain. When the aliphatic chain is lengthened to ten methylenes, polymers

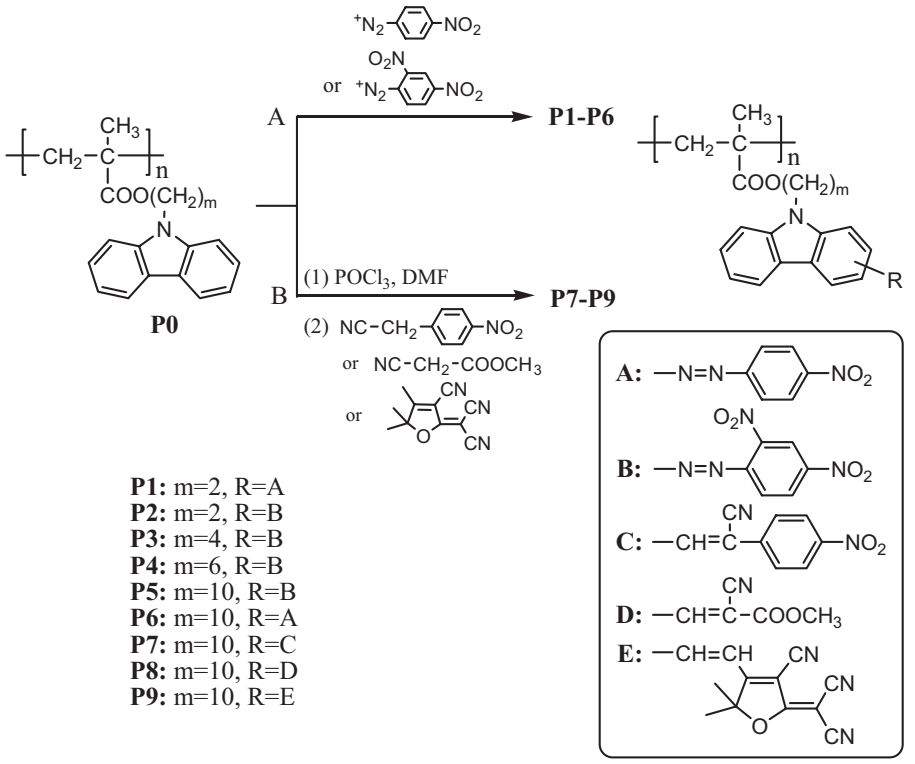

Scheme 5.
Polymethacrylates with different aliphatic spacer and PR chromophore.

Table 4.
Relative data to polymethacrylate with PR chromophore.

Polymer	λ_{max}/nm[a]	T_g/°C	NLO(mol%)[b]
P1	434	160	80
P2	468	182	77
P3	469	132	70
P4	470	125	30
P5	471	60	103
P6	437	36	30
P7	428	40	47
P8	401	58	63
P9	512	55	25

Note:[a]Measured from DMF solution with a mol concentration of 0.1 μmol/L by UV-vis spectroscopy; [b]Calculated from elemental analysis and ^{1}H-NMR spectra.

P5–**P9** have a lower T_g value from 36 °C-60 °C even if the strong electron-withdrawing group, tricyanofuran, is introduced as an acceptor onto carbazole. As shown in Table 4, their absorption maxima range from 401 nm to 512 nm due to the introduction of different acceptors. Notably, an excellent all-optical PR performance was obtained from undoped PR film of polymer **P6** without any plasticizer, photosensitizer and poling, and the coupling gain was measured by TBC to be 144 cm^{-1} at zero applied electric field as shown in Figure 4 (left) and its four-wave mixing diffraction efficiency was measured to be 8.3%. This is the best all-optical PR performance of all the PR polymers we synthesized. The all-optical PR performance of polymer **P6** has the same mechanism as hyperbranched organic monolithic molecular glass **CTP2**. The synergism of the longitudinal space charge field and the photoassisted poling of azo dye, which is derived from the repeated *trans-cis-trans* photoisomerization induced by a polarized light, leads to the all-optical TBC effect in polymer **P6** although the PR chromophore has been introduced into the side chain of NCMC polymers. The holographic image by the optic data storage experiment of polymer **P6** is illustrated in Figure 4 (right).

In view of the excellent all-optical PR performance of hyperbranched monolithic molecular glass **CTP2** and polymer **P6**, the same azo-based PR chromophore with a carbazole moiety is introduced as a PR chromophore into polyphosphazenes as shown in Scheme 6,[18,19] which exhibit high thermal and oxidative stability, optical transparency from 220 nm to the near-IR region of the backbone and the ease of synthesis.[20] It is well known that polyphosphazenes are flexible inorganic polymers bearing a nitrogen-phosphorous-alternating main chain because the isolated island-like electron cloud does not affect the free rotation of the N-P bond.[21] In other words, polyphosphazenes are not conjugated polymers although single bonds (N-P) and

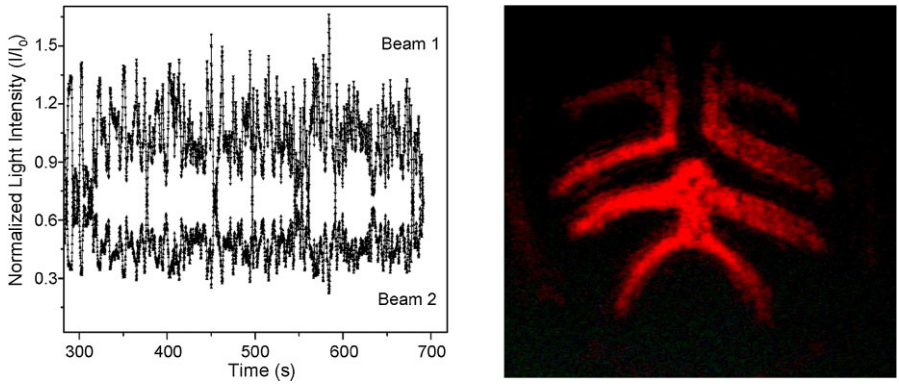

Figure 4.
TBC signal from nondoped PR film of **P6** at zero electric field without any photosensitizer and poling (left); holographic image from **P6** (right).

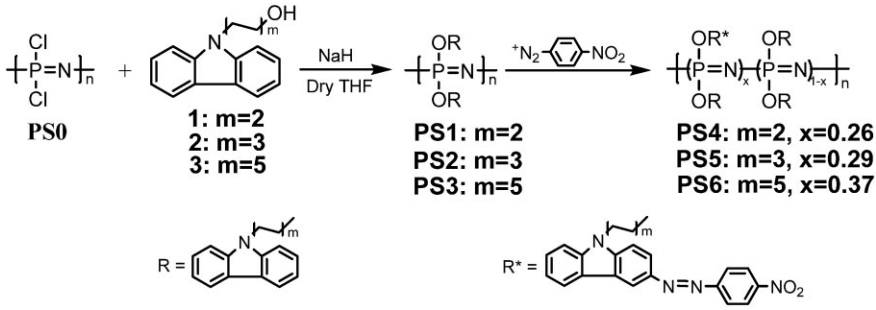

Scheme 6.
Polyphosphazenes with different aliphatic spacer and PR chromophore.

double bonds (N = P) are alternating in the polymeric main chain. Therefore, polyphosphazenes have the potential to obtain polymers with low T_g because the flexible skeleton affords the low-temperature elasticity. Polymer **PS0**, poly(dichlorophosphazene), was firstly prepared via ring-opening polymerization from hexachlorocyclotriphosphazene. Then, polyphosphazenes **PS1**, **PS2** and **PS3** with a carbazole moiety were subsequently prepared by the substitution of chloro groups in polymer **PS0** with a carbazole compound, *N*-hydroxylethylcarbazole. Finally, polyphosphazenes **PS4**, **PS5** and **PS6** were obtained via a post-azo-coupling reaction, in which the carbazole ring is partially functionalized with a nitrophenyl azo group. The content of NLO chromophore in polyphosphazenes **PS4**, **PS5** and **PS6** increases from 26% to 37% due to the weaker steric hindrance with lengthening of the aliphatic chain. Consequently, PR polyphosphazenes **PS4**, **PS5** and **PS6** have exactly a low T_g value varying from 20 °C to 65 °C. The TBC measurement from undoped PR films without any plasticizer, photosensitizer and poling showed us that the coupling gain of polyphosphazenes **PS4**, **PS5** and **PS6** are 50 cm^{-1}, 79 cm^{-1} and 91 cm^{-1} respectively at zero electric field. The all-optical TBC signal of **PS6** is given as an example in Figure 5.

Two series of PR polymers depicted above, both polymethacrylates and polyphosphazenes with PR chromophores, were also synthesized through a postfunctionalization strategy.[22] Although this approach has some advantages such as preparing functionalized polymers with high molecular weight, decreasing the amount of rigid chromophore groups which is beneficial to increase the ductility of the materials, tuning the content of PR chromophore and so on, it is impossible for functional group to be introduced into every repeating unit of the precursor polymers, i. e. the content of PR chromophore can not reach 100%. In addition, the definite chemical structure of PR polymers is almost impossible to be achieved as the reactive position is statistically existed in the precursor polymers. Therefore, it is a significant task to synthesize multifunctionalized PR polymers with high molecular weight and well-

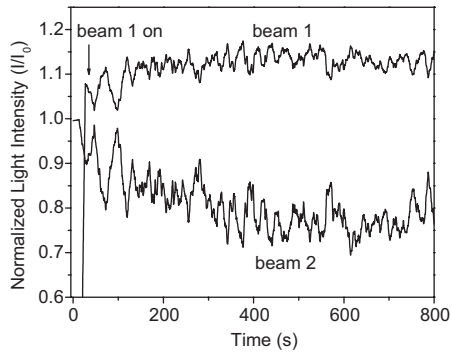

Figure 5.
TBC signal measured at zero electric field from non-doped PR film of **PS6** without any photosensitizer and poling.

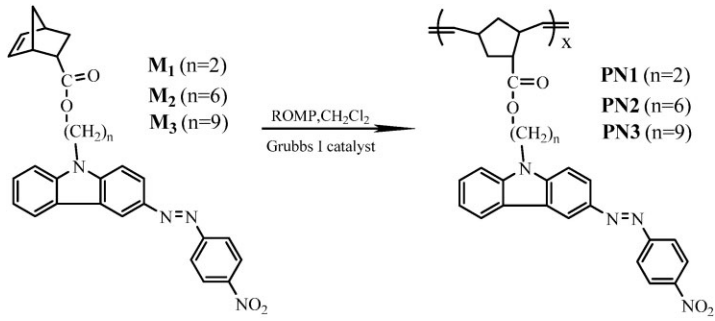

Scheme 7.
Polynorbornenes with different aliphatic spacer and PR chromophore.

defined structure through a simple synthetic strategy. Recent development in ring-opening metathesis polymerization (ROMP) of cyclic olefinic derivatives provides an excellent approach, especially the ROMP of norbornene functional monomers.[23,24] In order to obtain the all-optical PR polymers with well-defined chemical structure and chromophore content of 100%, multifunctionalized NCMC PR polynorbornenes **PN1**, **PN2** and **PN3** were synthesized as shown in Scheme 7 by the direct polymerization of functionalized monomers via ROMP of norbornene monomers containing a carbazole-based multifunctional PR chromophore using Grubbs I catalyst. Due to the existence of cyclopentane in every repeating unit, which blocks the free rotation of polymeric main chain, PR polynorbornenes **PN1**, **PN2** and **PN3** have a higher T_g value from 75 °C to 153 °C as listed in Table 6. In order to facilitate the PR measurement in room temperature, optically transparent films were fabricated with *N*-ethyl-carbazole (ECZ) as a plasticizer and C_{60} as a charge generator. These PR polymeric composites from polynorbornenes **PN1**, **PN2** and **PN3** have a lower T_g of 42 °C, 36 °C and 24 °C, respectively. Their photorefractive performance was evaluated at 633 nm by TBC experiment at a zero electrical field. All-optical TBC signals were observed from these PR films of the synthesized NCMC polynorbornenes without poling. The coupling gains of PR polymeric composites of polynorbornenes **PN1**, **PN2** and **PN3**, are 86 cm^{-1}, 53 cm^{-1}, 39 cm^{-1} respectively as shown in Table 6. The TBC signal from the PR film of **PN1** with ECZ of 30% and C60 of 1% at zero electric field without poling is given in Figure 6. Evidently, the present PR polynorbornenes have a high T_g and their coupling gain is not good enough. These will be further improved by appropriate molecular design in the future.

Table 5.
Relative data to polyphosphazenes with PR chromophore.

Polymer	λ_{max}/nm	T_g/°C	NLO (mol%)[a]	Γ_{633}/cm^{-1} (V/μm)[b]
PS4	433	65	26	50
PS5	433	50	29	79
PS6	435	20	37	91

Note:[a]the average number of NLO chromophores per repeat unit (-P=N-);[b]Measured at zero electric field from nondoped PR films without any photosensitizer and poling.

Table 6.
Relative data to polynorbornenes with PR chromophore.

Polymer	λ_{max}/nm	T_g^1 (°C)	T_g^2 (°C)	Γ_{633}/cm^{-1} [a]
PN1	440	153	42	86
PN2	432	103	36	53
PN3	441	75	24	39

Note: T_g^1 is the glass transition temperature of the polymers; T_g^2 is the glass transition temperature of the polymer composites;[a]Measured from PR films with 30 wt% ECZ and of 1 wt% C60 at zero electric field without poling.

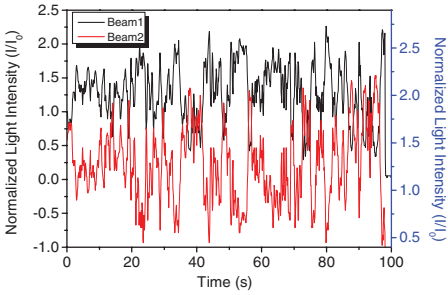

Figure 6.
TBC signal from PR film of **PN1** with 30 wt% of ECZ and 1 wt% of C60 at zero electric field without poling.

Outlook

Organic all-optical PR materials will soon become an interesting topic owing to the convenient signal-writing without the application of any external electrical field and poling although their PR performance is a little poorer than that under external electric field in most cases. In this paper, organic all-optical PR materials including organic monolithic PR molecular glasses and PR polymers synthesized in our laboratory have been systematically characterized. Much progress has been made not only in the synthesis strategy of organic all-optical materials but also in the primary mechanism of all-optical PR effect in organic materials. Even if the all-optical PR effect of organic azo-based PR materials is basically attributed to the synergism of the longitudinal space charge field and the photoassisted poling of azo dye from the repeated *trans-cis-trans* photoisomerization induced by a polarized light, for example, hyperbranched organic monolithic molecular glasses **CTP1** and **CTP2**, three series of PR NCMC polymers polymethacrylate, polyphosphazene and polynorbornene, the all-optical PR mechanism of organic PR materials is not yet understood completely, especially for organic methine-containing PR materials such as compounds **TPA1** and **TPA2**. However, it is believed that the specific orientation and grating formation of PR chromophore without external electric field and poling, even without any additives including plasticizers, photosensitizers and so on, will be understood well with further studies on all-optical PR effect of organic materials. These significant outcomings will broaden the application areas of organic PR materials.

Acknowledgements: We are grateful to the financial support from the National Natural Science Foundation of China (Project No. 20274042), the Henan Provincial Government of China (Project 2005HANCET-11), and the Fundamental Research Funds for the Central Universities (Project No.65010961).

[1] O. Ostroverkhova, W. E. Moerner, *Chemical Reviews* **2004**, *104*, 3267.
[2] D. Day, M. Gu, A. Smallridge, *Advanced Materials* **2001**, *13*, 1005.
[3] S. Tay, P.-A. Blanche, R. Voorakaranam, P. Voorakaranam, A. V. Tunc, W. Lin, S. Rokutanda, T. Gu, D. Flores, P. Wang, G. Li, P. St Hilarire, J. Thomas, R. A. Norwood, M. Yamamoto, N. Peyghambarian, *Nature* **2008**, *451*, 694.
[4] M. Talarico, A. Golemme, *Nature Materials* **2006**, *5*, 185.
[5] S. R. Marder, B. Kippelen, A. K.-Y. Jen, N. Peyghambarian, *Nature* **1997**, *388*, 845.
[6] G.-G. Francisco, D. M. Francisco, M. Klaus, *Nature Materials* **2008**, *7*, 490.
[7] A. Q. Jose, M. V. Jose, G. B. Pedro, *et al., Advanced Functional Materials* **2009**, *19*, 428.
[8] J. Shi, M. M. Huang, Y. R. Xin, Z. J. Chen, Q. H. Gong, S. G. Xu, S. K. Cao, *Materials Letters* **2005**, *59*, 2199.
[9] L. Zhang, S. G. Xu, Z. Yang, S. K. Cao, *Materials Chemistry and Physics* **2011**, *126*, 804.
[10] L. Zhang, J. Shi, Z. W. Jiang, M. M. Huang, Z. J. Chen, Q. H. Gong, S. K. Cao, *Advanced Functional Materials* **2008**, *18*, 362.
[11] C. Barrett, B. Choudhury, A. Natansohn, P. Rochon, *Macromolecules* **1998**, *31*, 4845.
[12] M. Ho, C. Barrett, J. Paterson, M. Esteghamatian, A. Natansohn, P. Rochon, *Macromolecules* **1996**, *29*, 4613.
[13] E. Hattemer, R. Zentel, E. Mecher, K. Meerholz, *Macromolecules* **2000**, *33*, 1972.
[14] Y. Liu, Y. Sui, J. Yin, J. Gao, Z. Zhu, D. Huang, Z. Wang, *Journal of Applied Polymer Science* **2000**, *76*, 290.
[15] J. Shi, Z. W. Jiang, S. K. Cao, *Reactive & Functional Polymers* **2004**, *59*, 87.
[16] J. Shi, M. M. Huang, Z. J. Chen, Q. H. Gong, S. K. Cao, *Journal of Materials Science* **2004**, *39*, 3783.
[17] J. Shi, Y. R. Xin, L. Zhang, S. G. Xu, S. K. Cao, *Reactive & Functional Polymers* **2005**, *62*, 223.

[18] L. Zhang, J. Shi, Z. Yang, M. M. Huang, Z. J. Chen, Q. H. Gong, S. K. Cao, *Polymer* **2008**, *49*, 2107.
[19] L. Zhang, M. M. Huang, Z. W. Jiang, Z. Yang, Z. J. Chen, Q. H. Gong, S. K. Cao, *Reactive & Functional Polymers* **2006**, *66*, 1404.
[20] H. R. Allcock, R. Ravikiran, M. A. Olshavsky, *Macromolecules* **1998**, *31*, 5206.
[21] H. R. Allcock, M. N. Mang, A. A. Dembek, K. J. Wynne, *Macromolecules* **1989**, *22*, 4179.
[22] H. Y. Pei, W. Li, Y. L. Liu, D. F. Wang, J. Wang, J. Shi, S. K. Cao, *Polymer* **2012**, *53*, 138.
[23] C. J. Hawker, K. L. Wooley, *Science* **2005**, *309*, 1200.
[24] R. H. Grubbs, *Advanced Synthesis & Catalysis* **2007**, *349*, 34.

